

Simulation and Defect Identification of Eddy-Current Induced Thermography

C.He*, Y.P Tian* ,S.S Wang* ,T.Y.Li*, J.Y.Xu*, X.J.Tian*, K.Y.Zhou**

* Department of Measuring and Testing Technology ,Nanjing University of Aeronautics and Astronautics,
Nanjing, China yptian@nuaa.edu.cn

** Department of Structural Engineering and Mechanics , Nanjing University of Aeronautics and
Astronautics, Nanjing, China zhoukeyin@nuaa.edu.cn

Abstract:

Pulsed eddy current (PEC) induced thermography is a new inspection technique which allows the user to capture the eddy current distribution in a component or structure using infrared imaging. PEC thermography is an emerging integrative nondestructive approach for the detection and characterization of surface and subsurface cracks. In this paper, heating behaviors of surface and subsurface cracks, excited by pulsed eddy current, are examined using numerical simulation. The varied models with edge , sub-surface and different angle shape cracks are built, which give the temperature distribution graphic pattern of different defects formed by eddy current, and defect identification is achieved according to the patterns. Some experiment results are given for comparison.

1. Introduction

Induction thermal excitation involves lots of complicated physical processes, such as electromagnetic induction, heat conduction and interaction. Numerical computation is widely used in the analysis of those processes. Activated by electromagnetic induction, thermal image of the test piece is acquired by the infrared imager, and the thermal radiation of the surface of the test piece is decided by the interaction of induction heating and thermal transmission. COMSOL, multiphysics finite element simulation software , is used for building infrared induction activated models and analyzing the processes of induction heating and heat transfer. 3D electromagnetic field model is built by the Electro-Thermal Heating of the AC/DC module. By analyzing those simulation models, the non-destructive testing method of induction-activated thermography is introduced.

The simulation model built for induction-activated thermography is composed of three parts of coil, test piece and shield. The coil is designed as a round one in this paper, which is activated by high-frequency impulse signal. Calculation of the model includes induction heating and heat transfer. Material parameters and boundary conditions of both processes should be installed. The paper puts emphasis on the temperature variation of the domain and section and the distribution of flux lines.

In this paper the induction-activated thermography is studied from aspects of simulation and experimental analysis. The different models with edge , sub-surface and different angle shape cracks are built respectively, and the temperature distribution of different defects formed by eddy current are given. We summarize the morphology of different defects by analyzing the heat distribution on the surface of the test piece.

2.Simulation modeling of cracks

2.1 Simulation modeling of edge cracks

The edge crack is easily formed since stress is concentrated on the edge. Usually, it is hard to detect and extract edge crack. The simulation and calculation follow show the advantages of induction-activated thermograph in detection of edge crack with fast, intuitional and non-contact.

The edge crack model is built by the Electro-Thermal Heating of the AC/DC module in COMSOL. An iron sample size of 20mm×20mm×5 mm with a rectangular crack size of 0.1mm×6mm is modeled. The depth of the edge crack is 1, 2, 3.....8mm respectively. The material properties are listed in Table.1.

Table.1 Thermal characteristics of iron

	Density	Thermal conductivity	Heat capacity	Electrical conductivity	Relative permeability
Iron	7780[kg/m ³]	76.2[W/(m*k)]	440[J/(kg*K)]	1.12e7[S/m]	4000

The circular energized coil is 5mm in radial with 50mm in external diameter and 40mm in inner diameter. As shown in figure 1 ,under the condition of coil current is 350A, in excitation frequency is 256kHz and excitation time is 200ms , a temperature distribution pattern is shown in Fig.1(a). Fig.1(b) give the eddy current distribution of crack with different depth h (1,2,3.....8mm).

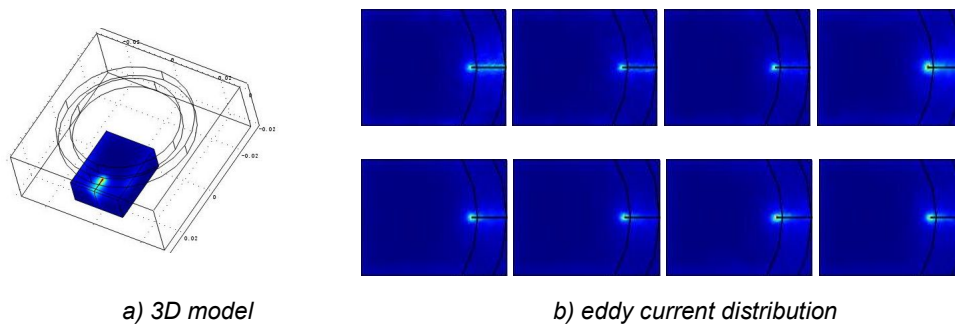
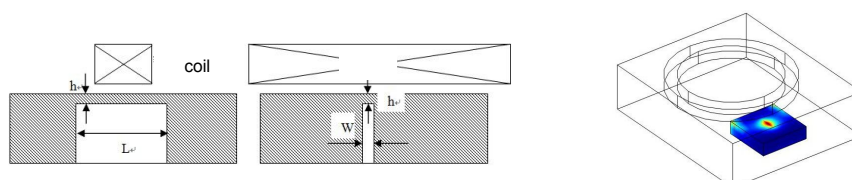


Fig.1 edge crack

2.2 Simulation modeling of subsurface cracks

Subsurface cracks sometimes happen and cause damage during the production process. A simulation model is built to see if the non-destructive testing method of induction-activated thermography applying to detect this crack. Pulsed eddy current excitation is applied on the test piece as shown in Fig.2.



(a) Schematic diagram

(b) 3D model

Fig.2 subsurface crack

The iron material and coil used are as above. The iron sample size of 20mm×20mm×5 mm with a rectangular crack in the middle of the test piece is modeled. The crack is 6mm in length. Three groups of subsurface cracks with width w (0.2mm,0.3mm,0.4mm) were examined, as shown in Fig.2(a), and each group has five cracks with distance h (0.1, 0.2, 0.3, 0.4, 0.5mm) from the surface respectively. The crack is right under the energized coil

The image shown in Fig.2(b) is the simulation result based on the subsurface crack model which is 0.2mm width and 0.1mm far from the surface. We can see heat generated at the top of the crack and temperature is higher in the center and gradually reduced around.

3. Simulation and analysis of the crack in different forms

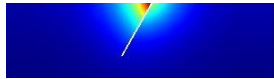




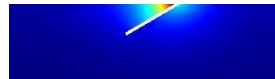
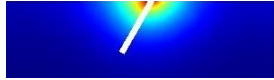

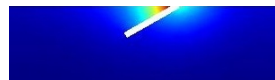

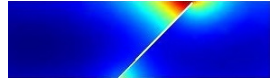







3.1 Simulation and analysis of inclined crack

Frequently varied cracks, both vertical cracks and inclined cracks, are appeared in the test piece. The inclined crack model under the electromagnetic induction is simulated and identification of the cracks is studied. Inclined crack models of surface and subsurface are examined as shown below. Three groups of surface cracks and three groups of subsurface cracks which are 0.1mm under the surface of the test piece, with varied inclination angles α (30°, 45°, 60°) and varied widths w (0.1, 0.2, 0.4mm) are examined. The simulation result is as shown in Table.3 and Table 4.

Table3. Simulation results of the inclined cracks

	Surface $w=0.1$	Surface $w=0.2$	Surface $w=0.4$	Subsurface $w=0.1$	Subsurface $w=0.2$	Subsurface $w=0.4$
Inclination $\alpha =30^\circ$						
Inclination $\alpha =45^\circ$						
Inclination $\alpha =60^\circ$						

Table4. Cross section of simulation results of the inclined cracks

	Inclination $\alpha = 30^\circ$	Inclination $\alpha = 45^\circ$	Inclination $\alpha = 60^\circ$
Surface $w=0.1$			
Surface $w=0.2$			
Surface $w=0.4$			
Subsurface $w=0.1$			
Subsurface $w=0.2$			
Subsurface $w=0.4$			

3.2 Simulation and analysis of more complex cracks

One or several cracks may arise during the production. To detect and distinguish complex cracks through eddy-induced thermography, several models of crisscross crack, T-end crack, cross crack are built.

Models of complicated crack of surface and subsurface are built for comparison. An iron sample size of 20mm*20mm*10mm is modeled with the complicated surface crack of 8mm-length and 5mm-depth . The other iron sample size of 20mm*20mm*5mm is modeled with a subsurface crack of 8mm in length and 0.1mm below the surface of the test piece. The energized circle coil ,with coil current is 350A, excitation frequency is 256kHz and excitation time is 200ms, is right above the crack parallel. Cross edge model and the temperature distribution patterns are shown in Fig.3 . Three groups of cracks with varied widths w (0.1mm/0.2mm/0.4mm) were examined, each group has four cracks with cross angle θ ($30^\circ/45^\circ/60^\circ/90^\circ$) respectively. Table 5 gives the stimulation results.

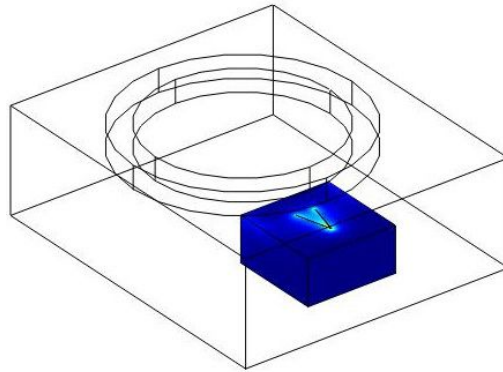
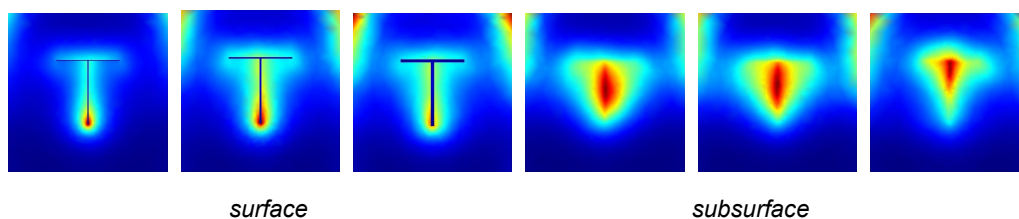


Fig.3 The cross crack model

Table 5 Simulation results of the cross cracks

	Surface w=0.1	Surface w=0.2	Surface w=0.4	Subsurface w=0.1	Subsurface w=0.2	Subsurface w=0.4
Cross $\theta = 30^\circ$						
Cross $\theta = 45^\circ$						
Cross $\theta = 60^\circ$						
Cross $\theta = 90^\circ$						

The image shown in Fig.4 is the simulation result of the T-end crack model. From left to right are the results of three surface cracks with varied widths w (0.1mm/0.2mm/0.4mm) and three subsurface cracks with varied widths w (0.1mm/0.2mm/0.3mm).



surface

subsurface

Fig.4 Simulation results of T-end crack

As shown in the Fig.4, the eddy current density and temperature variation reached to its maximum at the tip of the crack (the bottom of T) in the surface edge model. As the width increases, the temperature distribution and the current density of the tip and edge of the crack becomes equal. As shown in the results of the subsurface cracks, the temperature variation reached to its maximum right above the crack. The triangle temperature area of the internal defect is irregularly shaped.

The image shown in Fig.5 is the simulation result of the crisscross crack model. From left to right are the results of three surface cracks with varied widths $w(0.1\text{mm}/0.2\text{mm}/0.4\text{mm})$ and three subsurface cracks with varied widths $w(0.1\text{mm}/0.2\text{mm}/0.3\text{mm})$.

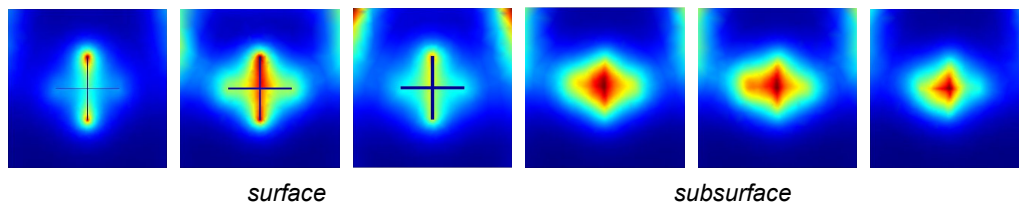


Fig.5 Simulation result of crisscross crack

Similar to the T-end model, for crisscross crack, the temperature variation reached to its maximum at the tip of the crack with the width of 0.1mm, and as the width increases, the temperature and eddy distribution of the tip and edge of the crack becomes equal. The eddy distribution is sensitivity to the angle between the crack and the coil. The eddy current density and temperature variation are greater at 90° than that at 0° . This should be considered during the detection of both surface crack and subsurface crack. Repeatedly detections based on different direction of coil and different angles can be taken to reduce this influence.

4. Analysis and identification of crack defects by experiment

Experiment is made on metal test specimen with surface cracks. The temperature distribution images of vertical cracks and inclined cracks are different under induction excitation. By graphic pattern comparing analysis of the different vertical cracks and inclined cracks, the identification of different cracks is realized in this paper.

For comparison, Fig.6 show the experimental results of vertical crack and inclined crack respectively. The crack depth is 8mm and width is 0.3mm. The inclination edge is 45° .

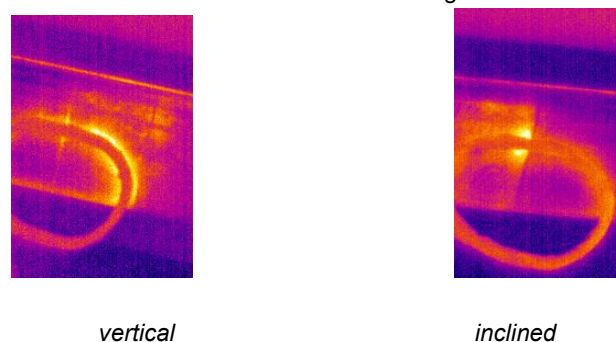


Fig.6 infrared thermal image of the vertical and inclined crack

An obvious temperature rising can be seen at the acute angle of the inclined crack test piece contrast to the other side, while the temperature rising is concentrated in the crack. Two models which are respectively has a 30° and 60° angle between the crack and the normal are shown in Fig.7 to make contrast on simulation and experiment.



Fig.7 Simulation result of inclined crack

The simulation results conform to the experimental results. The temperature variation area is bigger at the acute angle. And at the same size of inclined cracks, the temperature variation increases as the normal angle increases. Experimental result of varied depth h (2,4,8mm) cracks are show in Fig.8. For the same inclined edge(45°) the temperature variation area increases with decreasing of edge depth .

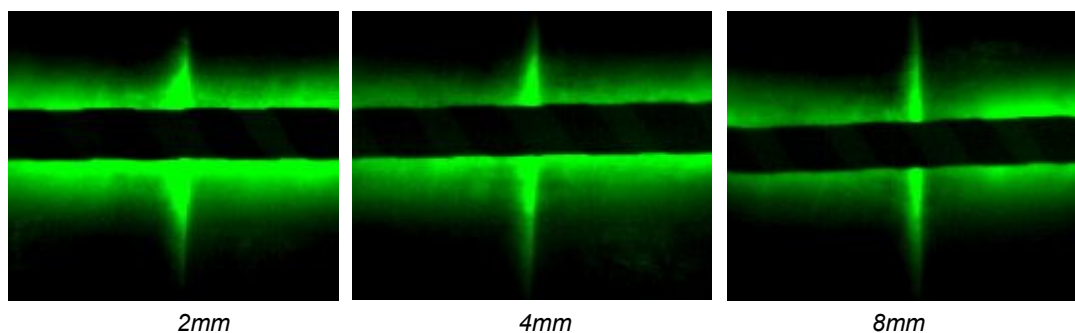


Fig.8 infrared thermal image of the same inclined crack with different depth

According to the results above, vertical cracks and inclined cracks have different image features. The temperature variation of the vertical crack is mainly concentrated in the crack, but for inclined crack, the temperature rising area appears in a small zone on the edge of the crack. The range of temperature variation at inclined cracks is larger than the vertical cracks. And the temperature rising area and the temperature variation increases with the increases of the inclination angle.

5. Conclusion

According to the experiment and simulation results of crack detection by induction-activated thermography above, several conclusions can be made. Different cracks leads to different temperature variation and temperature distribution image under the excitation of electromagnetic induction. As is

referred above, a crack with width less than 0.2mm and depth more than 2mm leads to a spot of temperature rising on the tip of the crack in the image, while a vertical crack with width over 0.2mm leads to a bar area of temperature variation. A small area of temperature rising can be suspected in inclined crack and subsurface crack, and then the type of the crack can be judged by the amplitude of the temperature variation. The relation between the area of the temperature rising part with the depth and inclination of the crack is needed to be further studied. The temperature distribution can also be changed with the crack size. Further experiments and simulation are needed for the quantification inspection of the crack.

(A project is funded by The national science and technology pillar program: project No:2012BAA01B02, FP7-PEOPLE-2010-IRSES, Grant agreement number:269202)

Reference

- [1] N.Tsopelas, N.J.Siakavellas, Performance of circular and square coils in electromagnetic-thermal non-destructive inspection[J], *NDT&E International*, 40(2007):12–28.
- [2] Netzelmann U, Walle G. Induction thermography as a tool for reliable detection of surface defects in forged components[C]. 17th World Conference on Nondestructive Testing. Shanghai, China: 2008.
- [3] J. Wilson, G. Y. Tian, I. Z. Abidin, et al. Modelling and evaluation of eddy current stimulated thermography[J], *Nondestructive Testing and Evaluation*, 2010, 25:205-218.
- [4] Reimche, W Bernard, M Bombosch, et al. Detection of incipient cracking in the edge region of high performance components using eddy-current technology and induction-activated thermography[J]. *Journal of Heat Treatment and Materials*. 2008, 63(5) 284-297.
- [5] G. Zenzinger, J. Bamberg, W. Satzger, et al. Thermographic crack detection by eddy current excitation[J], *Nondestructive Testing and Evaluation*, 22(2–3), 2007, 101–111.
- [6] B.Oswald-Tranta. Thermo-inductive crack detection[J], *Nondestructive Testing and Evaluation*, 22(2-3), 2007, 137-153.
- [7] J.D. Lavers. State of the art of numerical modeling for induction processes[J]. *The International Journal for Computation and Mathematics in Electrical and Electronic Engineering*, 2008, 27(2): 335~349.
- [8] S. Yang, G. Y. Tian, I. Z. Abidin, et al. Simulation of edge cracks using pulsed eddy current stimulated thermography[J], *Journal of Dynamic Systems, Measurement, and Control*, 2011, 133.
- [9] J.Wilson, G.Y.Tian, I Z Abidin, et al. Pulsed eddy current thermography: system development and evaluation[J]. *Insight-Non-Destructive Testing and Condition Monitoring*, 2010, 52 (2): 87-90.
- [10] G.Y. Tian, J.Wilson, L.Cheng, et al. Pulsed Eddy Current Thermography and Applications[M]. *New Developments in Sensing Technology for Structural Health Monitoring*, 2011, 205-231.